

AD _____

CONTRACT NO: DAMD17-94-C-4047

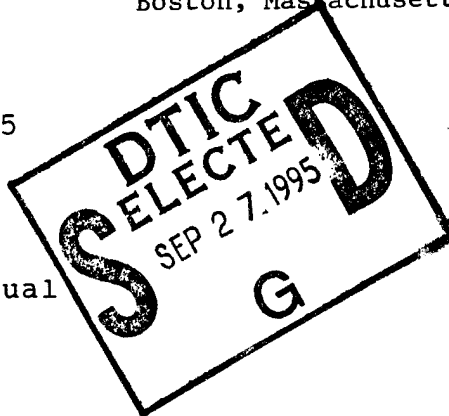
TITLE: Crystallographic Studies of the Anthrax Lethal Toxin

PRINCIPAL INVESTIGATOR: Robert C. Liddington, Ph.D.

CONTRACTING ORGANIZATION: Dana-Farber Cancer Institute
Boston, Massachusetts 02115

REPORT DATE: 7/27/95

TYPE OF REPORT: Annual



19950925 141

PREPARED FOR: U.S. Army Medical Research and
Materiel Command
Fort Detrick, MD 21702-5012

DISTRIBUTION STATEMENT: Approved for public release;
distribution unlimited

The views, opinions and/or findings contained in this report are those of the author(s) and should not be construed as an official Department of the Army position, policy or decision unless so designated by other documentation.

DTIC QUALITY INSPECTED 5

REPORT DOCUMENTATION PAGE

Form Approved
OMB No. 0704-0188

Public reporting burden for this collection of information is estimated to average 1 hour per response, including the time for reviewing instructions, searching existing data sources, gathering and maintaining the data needed, and completing and reviewing the collection of information. Send comments regarding this burden estimate or any other aspect of this collection of information, including suggestions for reducing this burden, to Washington Headquarters Services, Directorate for Information Operations and Reports, 1215 Jefferson Davis Highway, Suite 1204, Arlington, VA 22202-4302, and to the Office of Management and Budget, Paperwork Reduction Project (0704-0188), Washington, DC 20503.

1. AGENCY USE ONLY (Leave blank)		2. REPORT DATE 7/27/95	3. REPORT TYPE AND DATES COVERED Annual, July 1, 1994 - June 30, 1995
4. TITLE AND SUBTITLE Crystallographic Studies of the Anthrax Lethal Toxin			5. FUNDING NUMBERS DAMD17-94-C-4047
6. AUTHOR(S) Robert C. Liddington, Ph.D.			
7. PERFORMING ORGANIZATION NAME(S) AND ADDRESS(ES) Dana-Farber Cancer Institute Boston, Massachusetts 02115			8. PERFORMING ORGANIZATION REPORT NUMBER
9. SPONSORING/MONITORING AGENCY NAME(S) AND ADDRESS(ES) U.S. Army Medical Research and Materiel Command Fort Detrick, MD 21702-5012			10. SPONSORING/MONITORING AGENCY REPORT NUMBER
11. SUPPLEMENTARY NOTES			
12a. DISTRIBUTION / AVAILABILITY STATEMENT Approved for public release; distribution unlimited			12b. DISTRIBUTION CODE
13. ABSTRACT (Maximum 200 words) The lethal form of Anthrax results from the inhalation of anthrax spores. Death is primarily due to the effects of the lethal toxin (Protective Antigen (PA) + Lethal Factor) from the causative agent, <i>Bacillus anthracis</i> . All the Anthrax vaccines currently in use or under development contain or produce PA, the major antigenic component of anthrax toxin, and there is a clear need for an improved vaccine for human use. The work described in this report defines for the first time the atomic resolution structure of PA, revealing the domain structure of the molecule and the precise residues involved in each of the four domains. Together with existing biochemical and genetic data, we have begun to assign functions to each domain, although some of these assignments must remain speculative until the crystal structure of the oligomeric form of the protein (PA63) has been determined. This information can be used in the construction of recombinant domain fragments and mutant proteins that lack many of the key functions of the parent protein, but are highly immunogenic and have improved therapeutic properties as vaccines.			
14. SUBJECT TERMS Anthrax, Protective Antigen, Vaccine			15. NUMBER OF PAGES 27
			16. PRICE CODE
17. SECURITY CLASSIFICATION OF REPORT Unclassified	18. SECURITY CLASSIFICATION OF THIS PAGE Unclassified	19. SECURITY CLASSIFICATION OF ABSTRACT Unclassified	20. LIMITATION OF ABSTRACT Unlimited

FOREWORD

Opinions, interpretations, conclusions and recommendations are those of the author and are not necessarily endorsed by the US Army.

N/A X Where copyrighted material is quoted, permission has been obtained to use such material.

N/A X Where material from documents designated for limited distribution is quoted, permission has been obtained to use the material.

N/A X Citations of commercial organizations and trade names in this report do not constitute an official Department of Army endorsement or approval of the products or services of these organizations.

N/A X In conducting research using animals, the investigator(s) adhered to the "Guide for the Care and Use of Laboratory Animals," prepared by the Committee on Care and Use of Laboratory Animals of the Institute of Laboratory Resources, National Research Council (NIH Publication No. 86-23, Revised 1985).

N/A X For the protection of human subjects, the investigator(s) adhered to policies of applicable Federal Law 45 CFR 46.

AB ✓ In conducting research utilizing recombinant DNA technology, the investigator(s) adhered to current guidelines promulgated by the National Institutes of Health.

AB ✓ In the conduct of research utilizing recombinant DNA, the investigator(s) adhered to the NIH Guidelines for Research Involving Recombinant DNA Molecules.

N/A X In the conduct of research involving hazardous organisms, the investigator(s) adhered to the CDC-NIH Guide for Biosafety in Microbiological and Biomedical Laboratories.

265 L. H. S. 7/27/95
PI - Signature Date

Table of contents

Front Cover	i
SF298	ii
Foreword	iii
Table of contents.	iv
Introduction.	1
Body.	4
Conclusions:	17
References.	18
Bibliography.	23

Accession For	
NTIS CRA&I	<input checked="" type="checkbox"/>
DTIC TAB	<input checked="" type="checkbox"/>
Unannounced	<input type="checkbox"/>
Justification	
By	
Distribution /	
Availability Codes	
Dist	Avail and/or Special
A-1	

CRYSTALLOGRAPHIC STUDIES OF THE ANTHRAX LETHAL TOXIN

INTRODUCTION

1. Background

Anthrax is primarily a disease of herbivorous animals, particularly sheep and cattle (1). Humans may acquire the disease from infected animals, typically as a cutaneous infection characterized by black pustules (2). The pulmonary infection results from the inhalation of anthrax spores, as a result of handling contaminated animal hides or from the release of man-made stores (16,17), and can lead to death within days (3-5). The causative agent of anthrax is the gram-positive, aerobic, spore-forming *Bacillus anthracis* (6). The pathogenesis of *B. anthracis* depends on two major virulence determinants: 'anthrax toxin', and an antiphagocytic poly(D-glutamic acid) capsule, each encoded by a separate plasmid (see (7) for a general review). The term 'anthrax toxin' refers collectively to three proteins of similar molecular weight, encoded by plasmid pXO1: Lethal Factor (LF; 776 a.a.), Edema Factor (EF; 767 a.a.), and Protective Antigen (PA; 735 a.a.). The proteins lack toxicity when administered individually (8), but two binary combinations are toxic: co-injection of PA with EF ("edema toxin") produces edema in the skin of animals and inhibits the function of phagocytic cells (9), while the combination of PA and LF ("lethal toxin") induces death (10,11). The shock and death resulting from systemic anthrax are primarily due to the effects of the lethal toxin, as animals treated with lethal toxin show symptoms closely resembling those characterizing infection with the bacillus (12,13,14).

There is a clear need for an improved Anthrax vaccine for human use (15-17): the currently licensed vaccine in the United States, consisting of a cell-free filtrate of anthrax absorbed onto aluminum hydroxide, requires multiple doses, produces frequent side-effects, and is not effective against certain virulent strains. Much effort has been directed towards the goal of a human vaccine that is fully defined chemically, contains only essential ingredients, confers protection in a single dose, and has no side-effects. All the Anthrax vaccines currently in use or under development contain or produce Protective Antigen. Lethal Factor and Edema Factor have also demonstrated potential as protective immunogens, whereas structural components such as capsule, surface polysaccharide and surface proteins have not.

The work described here aims at determining the atomic resolution structure of the anthrax protective antigen in its monomeric and oligomeric forms. We

anticipate that the three-dimensional data derived will be beneficial in the development of the next generation of Anthrax vaccines. Our structural work, together with the biochemical and genetic work of our collaborators, should allow us to define the domain structures of PA involved in receptor binding, Lethal Factor binding, membrane insertion and translocation, and the biochemical basis of Lethal Toxin lethality. This information can be used in the construction of recombinant domain fragments and mutant proteins that lack, of course, many of the key functions of the parent protein, but are highly immunogenic and have improved therapeutic properties.

2. Intoxication by Anthrax

The three exotoxin proteins are the edema factor (EF), the lethal factor (LF), and the protective antigen (PA), collectively called "anthrax toxin" (18). In the "A-B" toxin nomenclature, PA is the B moiety and LF and EF are alternative A moieties. Anthrax toxin (in common with certain clostridial toxins) is classified as a binary A-B toxin because the two moieties exist as separate gene products, not as domains within a polypeptide (19). The mature anthrax toxin polypeptides have molecular weights in the range 83-90kDa, and their genes have been cloned and sequenced (20-23). Mediating the effects of lethal toxin is the macrophage. In vitro, only cells of the macrophage lineage are affected by exposure to lethal toxin (18): high concentrations lead to cytolysis (18,25), likely mediated by the overproduction of reactive free radical oxygen intermediates (26), while lower concentrations can induce cytokine overproduction (24), proposed to be the cause of the systemic shock and death associated with anthrax (24). In a recent study, Hanna and colleagues showed that mice depleted of macrophages are resistant to lethal-toxin challenge, and regain sensitivity upon injection of toxin-sensitive macrophages (24).

The events that occur during intoxication of the cell are as follows. The first step involves the binding of PA to a receptor on the host cell surface (12). The receptor is found in a variety of mammalian cell lines (12) and appears to be a membrane protein of 85-90 kDa with a high affinity for PA ($K_d \sim 1$ nM) (27). Once bound to the receptor, PA is cleaved by a cell-surface protease believed to be furin (28,29), a ubiquitous, subtilisin-like endoprotease (30). Proteolysis releases an N-terminal 20 kDa fragment, PA₂₀, from the cell surface (31) and exposes a high-affinity binding site ($K_d = 10$ pM) (7) for LF or EF on the 63 kDa fragment. PA₆₃, still attached to the receptor, then binds LF or EF, and the entire complex undergoes receptor-mediated endocytosis (32). Acidification of the vesicle leads to insertion of

PA₆₃ into the endosomal membrane (7) and translocation of EF or LF bilayer into the cytosol where they exert their toxic effects - adenylate cyclase activity in the case of EF (33), and (probably) proteolytic activity in the case of LF (34).

It has been recently shown that PA₆₃ forms a heptameric, ring-like structure in vitro (see below), which is probably the membrane-inserting form in vivo. It is not yet clear if oligomerization occurs at the cell surface or after acidification of the endosome, and the precise sequence of EF/LF binding, oligomerization and membrane insertion has yet to be established.

3. *The PA₆₃ Oligomer*

Leppla showed that following proteolytic cleavage of PA by trypsin in vitro, PA₆₃ associates into an SDS-resistant oligomeric structure which binds EF and LF with high affinity (12). Milne et al have recently shown that such an oligomer forms in mammalian cells and, judged by electron microscopy, is a heptamer (35). The oligomer appears as a compact ring made of seven subunits. Two domains can be distinguished, a larger one forming the body of the ring, and a smaller protrusion. The outer diameter of the rings is roughly 140 Å including the protrusions and 104 Å excluding them, while the inner diameter is 20 Å (35). In both artificial lipid bilayers (36-38) and cells (39), PA₆₃ inserts into membranes and forms ion-conductive channels. Channel formation in planar lipid bilayers is rapidly accelerated when the pH is lowered from 7.4 to 6.5 (36). In liposomes the formation of channels occurs at pH 6.0, is maximal at pH 4.7, and is only observed in the presence of a pH gradient (39). Although the precise pH requirements vary with experimental design, channel formation by PA₆₃ does not require as low a pH as does that by the B chains of diphtheria, tetanus and botulinum toxins (40). PA₆₃ channels appear to be selective for monovalent cations (36) and can be blocked by the addition of LF (41). Permeability to tetraheptylammonium ions indicates that the channel diameter is at least 12 Å (42-44), consistent with the electron microscopy. We have crystallized the heptamer in a water-soluble form at high pH, and have begun a full crystallographic analysis. This information should provide further data on those parts of the PA molecule which are exposed to solvent, and therefore further map the immunogenic surfaces of the molecule.

BODY

1. Crystallographic analysis

Data Collection, Model Building and Refinement of PA

Data were collected on our in-house system (Rigaku RU200 generator, graphite monochromator and Xuong-Hamlin multiwire detector), at the Stanford Synchrotron (MarResearch Imaging Plate) and at the Cornell Synchrotron (CCD detector). The structure of PA was determined by the conventional method of Multiple Isomorphous Replacement (MIR), using 6 heavy atom derivative (Table 1). Most of the work was done with a crystal form grown from PEG 1000; towards the end of the work a second crystal form was employed, grown from PEG 8000, that diffracted to higher resolution (2.1Å). Heavy atom positions were determined by inspection of Isomorphous Difference Pattersons and Difference Fourier. Heavy atom parameters were refined using the programs HEAVY (45) and MLPHARE (46). An initial model was built into an MIR map using the graphics program FRODO (47). The initial map was not of high quality, but various residue markers allowed for some stretches of the chain to be assigned; the iodine derivative labeled tyrosine residues, the cysteine point mutants were labeled with mercury, and the compound methylmercuric nitrate often bound to histidines. The large tryptophan sidechains were also clearly identified. However, most residues were initially modeled as polyalanine. The density corresponding to the stretch from Ser³³⁰ to Leu³⁹¹ was particularly well defined, and tracing was facilitated by the presence of the markers Trp³⁴⁶, Hg-labeled His³³⁶ and Hg-labeled Cys³⁵⁷ (in crystals of the point mutant T357C). The initial model consisted of 10 continuous polypeptide segments accounting for 524 residues and 2843 non-hydrogen atoms. The model was refined against the 15-2.5Å native data collected at the Stanford synchrotron using the program XPLOR (48). Simulated annealing (SA) was performed by heating the model to 1500 K and letting it cool in steps of 50K. The crystallographic R-factor (fractional discrepancy between observed and calculated model-derived data) after refinement was 0.437 for all reflections with $F_o > 2\sigma$. Phases were then calculated from the refined atomic coordinates to 3.2 Å resolution and recombined with the original MIR phases using the program SIGMAA (49). The new "recombined map" showed a marked improvement over the original MIR map. New density appeared, allowing for further residues to be modeled. Regions of density into which model had been correctly built were better defined, while those where errors had been made became less defined. Model in the poorer regions was removed and

Table 1: Crystallographic Statistics

	P2 ₁ 2 ₁ 2 ₁				P2 ₁ 2 ₁ 2 ₁			
	a=119.8 b=73.8 c=95.0				a=99.3 b=93.9 c=82.0			
	pH 7.5				pH 6.0			
	Native	MMN	MA	U	PtBr ₆ ⁻²	TTP	KI ₃	Native
Res. Limit (Å)	2.5	3.2	3.2	3.2	3.2	3.2	3.2	2.1
Unique observations	28421	11423	12768	12758	12073	10976	12541	49073
Completeness (%)	96	85	88	84	83	76	86	97
Multiplicity	3.3	4.2	2.4	3.1	2.6	3.0	4.0	3.9
R _{sym} (%)	6.6	4.7	5.0	5.7	7.0	5.2	7.5	9.3
Number of Sites		5	5	4	3	2	11	
R _{diff} (%)		8.9	13.0	11.0	13.9	12.5	13.1	
Phasing Power (Å)		1.1	0.7	0.5	0.9	0.6	0.6	
		(3.2)	(4.0)	(4.0)	(3.2)	(3.6)	(3.4)	
FOM (3.2 Å) Centric	0.74							
Acentric	0.58							
R-factor (%)	22.0							28.0
free R (%)	28.0							34.0
rms deviations								
			bond lengths	0.01 Å		bond angles	3.1°	

(without further refinement) new phases were calculated and recombined with the MIR phases. In this "omit-recombined map", the correct tracing was more apparent. The new model was then subjected to a second round of refinement, which reduced the R-factor to 0.419. New phases were calculated to 2.5 Å from this refined model and were combined with MIR phases previously modified and extended to 2.5 Å using the program SQUASH (50). This cycle of model-building, refinement and phase combination was iterated. In the initial rounds a conservative strategy was adopted during map interpretation by deliberately underestimating the electron density. Phe and Trp residues were placed where obvious, density consistent with medium-sized residues was modeled as Asn, and ambiguous density was modeled as polyAla, polyGly or not at all. After round 7, restrained B factor refinement was performed and higher temperatures were used in the simulated annealing. Maps inspected during the model building phase eventually included $2F_o - F_c$ maps, positively and negatively contoured $F_o - F_c$ maps, recombined maps, omit-recombined maps and SA-omit maps, calculated to 2.5 Å and to 3.2 Å. Successive rounds of the refinement/phase combination procedure led to the location of more and more sequence and to a gradually improving image of the molecule. The C-terminus was located quite early, marked by Phe⁷²⁷, iodine-labeled Tyr⁷³² and uranyl-labeled Glu⁷³³.

At this stage the model accounted for 709 of the 735 residues, of which 20 were modeled as glycine or alanine. The crystallographic and free R-factors to 2.5Å ($F_o > 2\sigma F_o$) were 23.4 % and 38.7%, respectively (no water molecules were placed at this stage). Some of the poorest electron density was in the interface between domains I and II (residues 159 to 219), so that the placement of domain I with respect to the rest of the molecule was uncertain, since two different positions related by crystallographic symmetry were feasible. To resolve this issue we pursued a different crystal form of PA, grown from PEG 8000 (15-20%), 50mM citrate pH 6. The space group is $P2_12_12_1$, with $a=101.Å$, $b=94.4Å$, $c=84.3Å$. Suitable flash freezing conditions were determined: 15% glycerol, 20% PEG8K, 50mM citrate. These crystals diffract better than the PEG 1000 form, and native data to 2.1Å resolution were collected from frozen crystals at the Cornell Synchrotron. The structure has been solved by the method of Molecular Replacement, using the atomic model of the first crystal form as the search object to be positioned into the new crystal. This newly positioned model has been refined, using simulated annealing with the program XPLOR to the resolution limit of the data. The R-factor is currently 29%. The addition of water molecules to this model should reduce the R-factor to an acceptable range (18-22%). On the basis of this new model, we are now confident of the domain boundaries and

the positions of all ordered residues in our model of the Protective Antigen (720 out of 735 amino-acids).

Cysteine point mutants

Leppa supplied us with 10 cysteine point mutants (the wild-type protein contains no cysteines). We attempted to crystallize these mutants and study crystals soaked in methylmercuric nitrate, initially in the hope that mercury would bind to cysteine and provide three-dimensional markers facilitating the chain trace. In two cases this was successful, and the data are summarized in Table 2. This information is described in detail since these mutants may be used by our collaborators to study the process of oligomerization and membrane insertion via spin-labeling. Three mutants failed to crystallize: S248 is buried, S278 is in an ordered loop that is involved in a crystal contact, and S249 in an exposed loop that forms part of a crystal contact.

Table 2: Cysteine point mutants

Mutant	Crystallizes?	Specific Hg-site?	Environment of residue	Residue found in
S170C	+	not tested	(not visible)	vicinity of cleavage site
S248C	-	N/A	partly buried	domain interface
S278C	-	N/A	crystal contact	ordered loop
F313C	+	-	(not visible)	disordered loop (302-24)
T357C	+	+	exposed	β strand
S429C	-	N/A	crystal contact	loop
T488C	+	-	buried	β strand
T548C	+	-	crystal contact	loop
S623C	+	+	exposed	β strand
S717C	+	not tested	exposed	loop

Seven mutants crystallized; five were of sufficient size for data collection: of these five three did not produce useful derivatives: F313 is in a disordered loop, T488 is buried and T548 is in an ordered loop that is involved in a crystal contact. Crystals of only two mutants, T357C and S623C, were able to bind a Hg atom in an ordered fashion, and our model demonstrates that residues 357 and 623 are on β -strands exposed to solvent. These studies suggest that most of the mutants are suitable for spin-label studies, and that the cysteines are available for derivatization (but either fail to crystallize due to proximity to a crystal contact or are too mobile to be seen crystallographically). The exceptions are S248, found at the domain1-2 interface; and T488 which is buried.

PA63 Oligomer

We have determined conditions for reproducibly seeding small crystals of PA63 in order to produce large crystals. The crystals have been fully characterized, and belong to space group $P2_1$, with $a=149\text{\AA}$, $b=141\text{\AA}$, $c=163\text{\AA}$, $\beta=105^\circ$, and diffract to about 4.5\AA resolution. The crystals are very radiation sensitive, so we have determined conditions for flash-freezing them and have collected a complete data set to 7.5\AA using our in-house facilities, and have begun heavy atom derivative searches. From the diffraction data it is possible to search for internal symmetry in the molecule before any heavy atom data are available. We have done this, using a "self-rotation function", and find that the PA63 molecule has a 7-fold axis of symmetry, and we calculate that the crystal contains about 70% solvent. This information confirms that PA63 crystallizes as a heptamer, which is the biologically active species that has been observed by electron microscopy and by studies of infected cells. On the basis of crystal packing analysis and electron microscopy measurements (39), we have built a hypothetical model for the heptamer (see below).

2. Three-dimensional Structure of the protective antigen (PA)

The molecule is about 100\AA tall by $50\text{-}70\text{\AA}$ wide and $30\text{-}40\text{\AA}$ deep (figure 1). The sequence with secondary structure assignments is shown in figure 2. It consists of four domains organized predominantly into β -sheets, with only a few short helices (≤ 4 turns long). The domain structures are discussed in detail below. Domains 1 and 2 are approximately equal in size, with ~ 250 residues each. Domain 1 contains PA20, the fragment removed by the cell surface protease. The function of domain 2 is not known, but it may play a role in membrane insertion and/or oligomerization. Domain 3 is the smallest of the domains with about 100 residues; its function is also currently

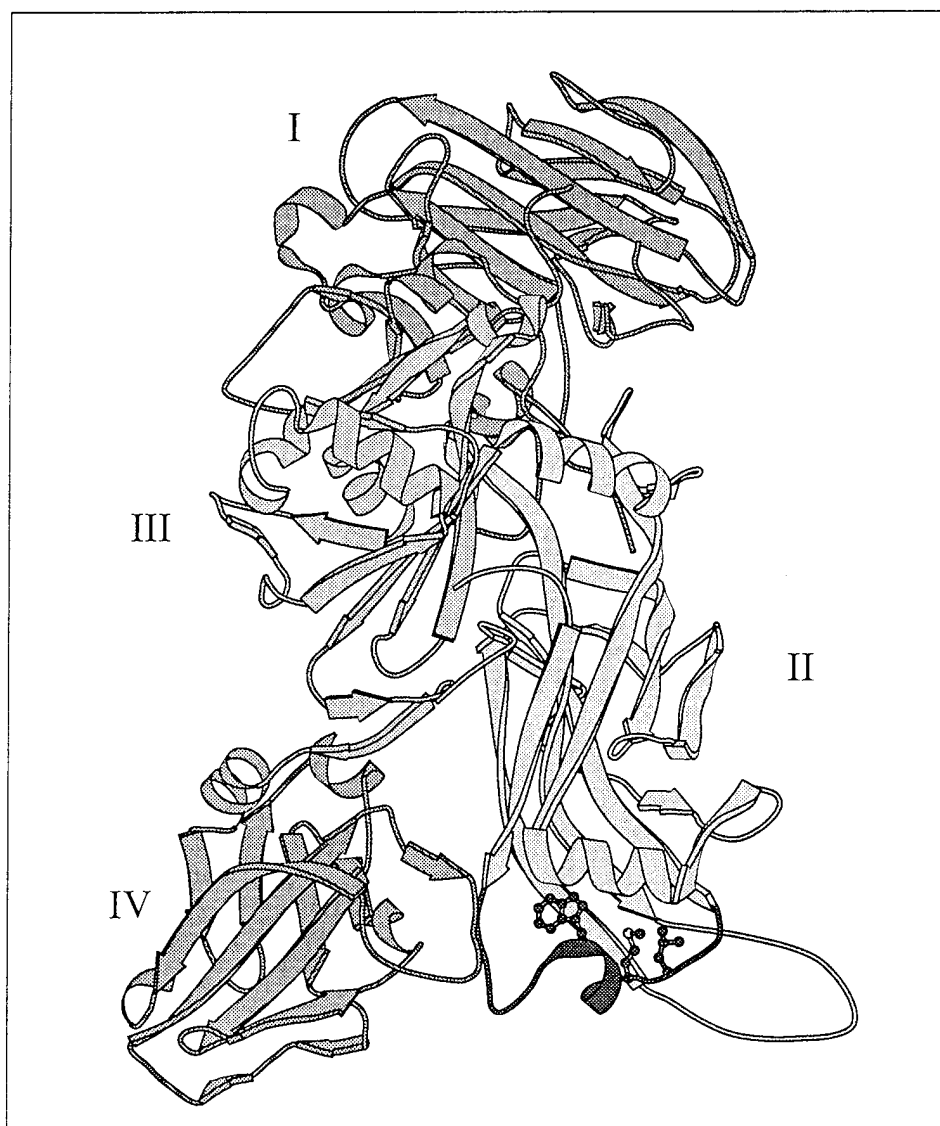


Figure 1: schematic structure of the Protective Antigen

unknown. Domain 4 contains the C-terminal 140 residues and is probably the receptor-binding domain.

Domain 1

Domain 1 consists of residues 1-249. Of these, the first 220 fold into 13 β -strands arranged in an antiparallel fashion in 2 sheets of unequal size. Protease cleavage on the cell surface occurs at the sequence RKKR¹⁶⁷ (51), which forms an exposed loop

between two strands of the larger sheet. Mutation of the cleavage site to prevent proteolysis results in a loss of toxic activity (52). Residues making up the PA₂₀ fragment form a β -sandwich composed of the small sheet and 6 of the 9 strands of the large sheet. That the cleavage site does not occur between structural domains but within a domain explains why it is possible to "nick" PA with trypsin without causing dissociation of the 2 resulting polypeptide chains (12). The remaining 3 strands of the large sheet (residues 190-220) pack against the last 30 residues of the domain, which seem to have little regular secondary structure. Domain 1 can thus be viewed as having 2 subdomains: (i) PA₂₀, which forms a 4+6 stranded β sandwich, and (ii) the remaining residues (168-249), which fold into a 3-stranded sheet and a random coil. Removal of PA₂₀ would not only disrupt hydrogen bonding interactions in this subdomain by tearing the large β -sheet, but would also cause several hydrophobic residues to become exposed. Perhaps this subdomain is poised to undergo a conformational change once PA₂₀ is removed. We do not yet know what functional role the residues in this subdomain play, but since PA cannot bind EF or LF until PA₂₀ is removed, they may be involved in EF/LF binding.

Domain 2

Domain 2 consists of residues 250-487 organized into a 9-stranded β -barrel and 2 α -helices located at either end of the barrel. The barrel contains three very long strands of contour lengths 39, 45 and 54Å, and a large loop made up of residues 304-321. The loop contains two hydrophobic residues at its tip, Phe-313 and Phe-314, and is susceptible to proteolysis by chymotrypsin (which cleaves after aromatic residues) (7,12). As in the case of the trypsin site of domain 1, it is possible to nick PA with chymotrypsin without causing dissociation into two fragments (12,51). However, this treatment renders the PA (in combination with LF) non-toxic to cells (51), despite its ability to bind to LF and to cell surface receptors, and to undergo receptor-mediated endocytosis (51). A deletion mutant lacking the two Phe residues was found to be defective in its ability to form oligomers (53). Taken together, these data suggest that the loop has a role in oligomerization and is probably involved in an intermolecular contact. A complementary surface has not yet been identified, but a strong candidate is an exposed hydrophobic patch located on the surface of domain 3, described below. The length of domain 2 (~50Å) would permit it to span a membrane.

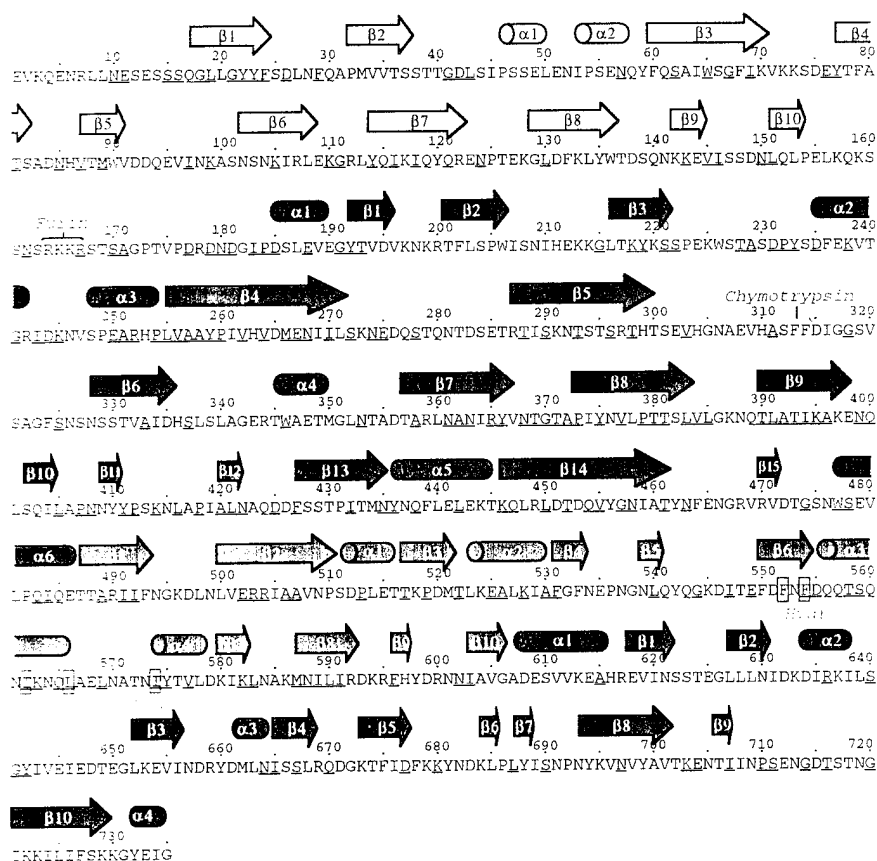


Figure 2: Sequence of PA with secondary structure assignments. Residues homologous with iota-toxin are underlined.

Domain 3

Domain 3 consists of residues 488-594 and is the smallest of the domains. It consists primarily of a 4-stranded β -sheet and 4 α -helices. One helix is part of a triangular strand-helix-loop structure that permits 5 hydrophobic residues to form a flat surface exposed to the solvent, constituting a "hydrophobic patch". In crystals of PA this patch is occupied by a phenylalanine residue from a neighbouring molecule. It is this interaction in the crystal that leads us to wonder whether, in an oligomer of PA₆₃, the hydrophobic patch of one monomer might be occupied by Phe-313 or -314 from domain 2 of a neighbouring monomer. Further studies are required to determine the significance of this patch and the functional role of the entire domain.

Domain 4

mutants have implicated domain 4 in receptor binding (54,55). Deletion of seven residues from the C-terminus leads to reduced toxicity, while deletion of 12 or 14 residues leads to complete loss of activity and sensitivity to proteases. The structure provides a rationale for these data: protein truncated at residue 728 would have half of the outer β -strand of a β -sheet missing; truncation at residue 723 would have all the final strand missing and severely affect the conformation and rigidity of the preceding loop between residues 704-722 which extends into the solvent and also forms part of the interface with domain 2.

While domains 1-3 appear quite intimately associated, domain 4 is much less so. The only contacts are the initial β -hairpin joining domain 4 with domain 3 and a small contact surface with domain 2. It is therefore conceivable that during membrane insertion (or perhaps at another step) domain 4 separates altogether from domain 2, swinging away to the left in figure 1.

Comparison of the two crystal forms

We have begun a detailed analysis of the two crystal forms. While the structures are very similar in most respects there are some small but fascinating differences. The two different crystal forms were obtained at different values of pH, the first at pH 7.5 and the second at pH 6. Two regions, consisting of residues 340-355 and 511-517 that are ordered in the pH 7.5 crystal form appear to be disordered at the lower pH. In the second case, a group of hydrophobic sidechains that was buried in the pH 7.5 form become exposed in the pH 6 form. This has potential biological significance, as it may represent a step in the pH-induced transformation from a water-soluble to a membrane-inserting molecule. We believe that these observations warrant further investigation to determine whether the changes we see are truly pH-induced or simply the product of different crystal environments.

Homology with Iota-Ib toxin

PA shares 34% sequence identity with the B-chain of the *Clostridium perfringens* iota toxin, another toxin whose A and B parts exist as separate polypeptides (56). Like PA, Iota-Ib is produced in a proform that is proteolytically activated and internalized by receptor-mediated endocytosis (57,58). Iota-Ib is believed to coordinate the delivery to the cytoplasm of the A moiety, iota-Ia, which

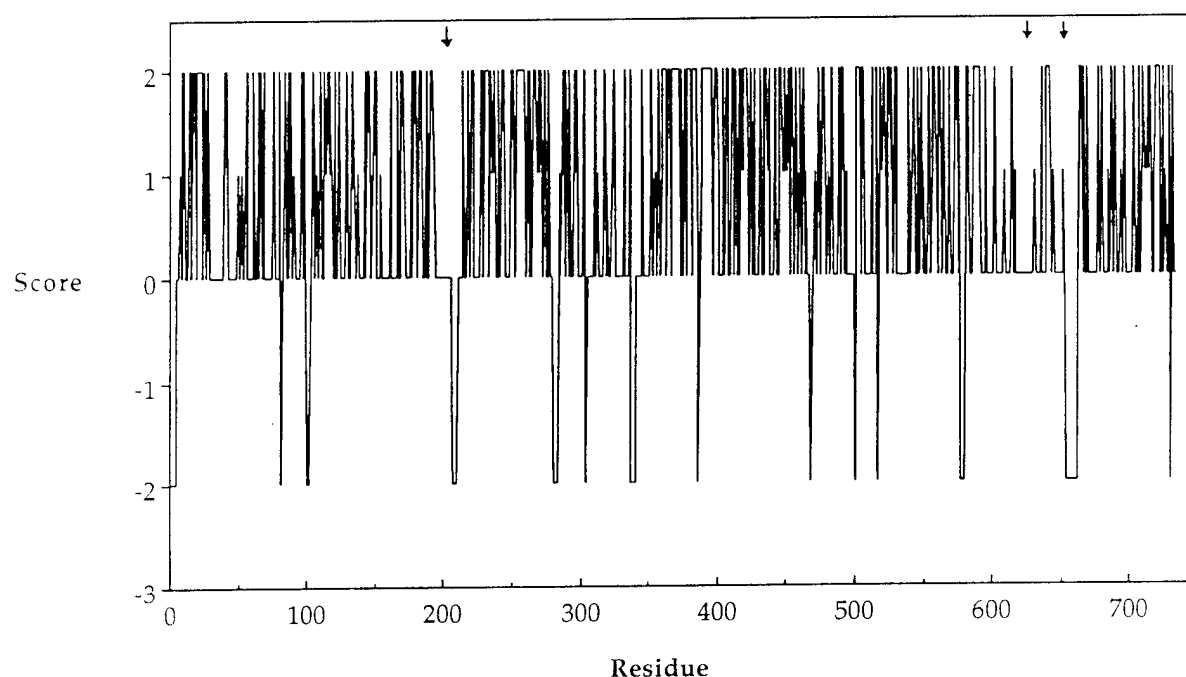


Figure 3: Homology between PA and iota-toxin (see text)

ADP-ribosylates actin (59-61) . Residues in PA identical to those in iota-Ib are underlined in figure 2. We assume that residues performing similar functions in PA and iota-Ib should exhibit a greater degree of similarity than those which interact with the receptors or with the A moieties, since these ligands differ for the two toxins. The highest degree of similarity occurs in the middle of the sequence (figures 2 and 3): domains 2 and 3 have 40 and 37% sequence identity, while domains 1 and 4 have 29 and 21% identity, respectively. Four of the five residues making up the hydrophobic patch of domain 3 have identical corresponding residues in iota-Ib, and the fifth, Phe-552, corresponds to a leucine. Thus, a hydrophobic patch likely also exists in iota-Ib. In general, the high homology of domains 2 and 3 is consistent with a putative role in oligomerization and membrane insertion.

Absence of homology is better illustrated in figure 3, in which each PA residue is assigned a score based on similarity to the corresponding iota-Ib residue. A score of 2 is given for identical residues, 1 for very similar residues (e.g. ile vs. leu, glu vs. asp), -2 for residues missing in the iota-Ib sequence, and 0 for all others. Three low-scoring regions, indicated by arrows, clearly stand out. Two stretches occur in domain 4, consistent with a role in receptor binding. The third and longest stretch occurs between residues 194-204, which are located in the 3-stranded b-sheet of

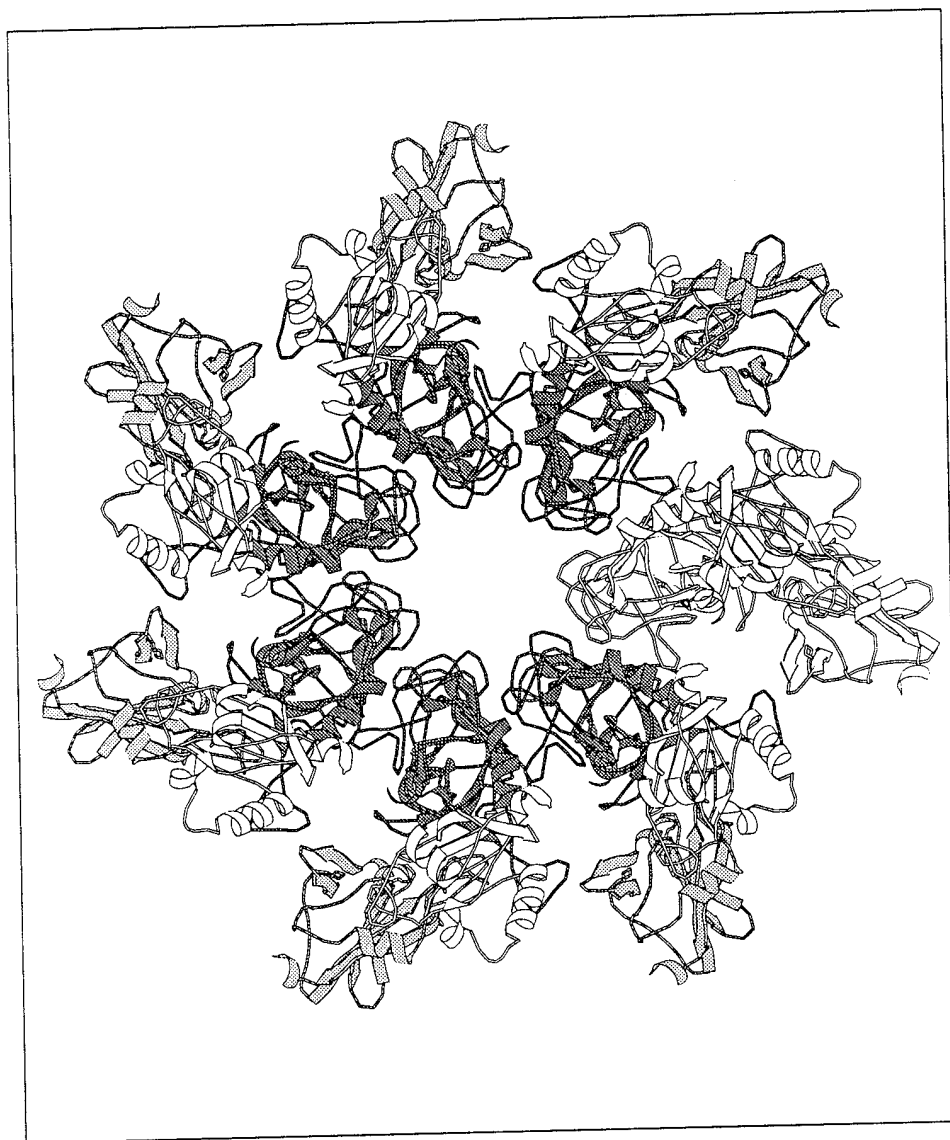


Figure 4a: *Hypothetical model of PA63: top view (see text)*

domain 1 (at the interface of PA20 and domain 2). The low degree of similarity in this region would be consistent with a role in EF/LF binding, since the A moieties in the two toxins show no homology.

A hypothetical model for oligomerization and membrane insertion

We have studied two crystal forms of PA, one obtained at pH 7.5 and the other at pH 6. The structure shown in figure 1 is that observed at pH 7.5, and closely resembles the low pH structure. The largest structural difference occurs in residues 242-255, located at the base of the barrel formed by domain 2. This region contains 3 hydro-

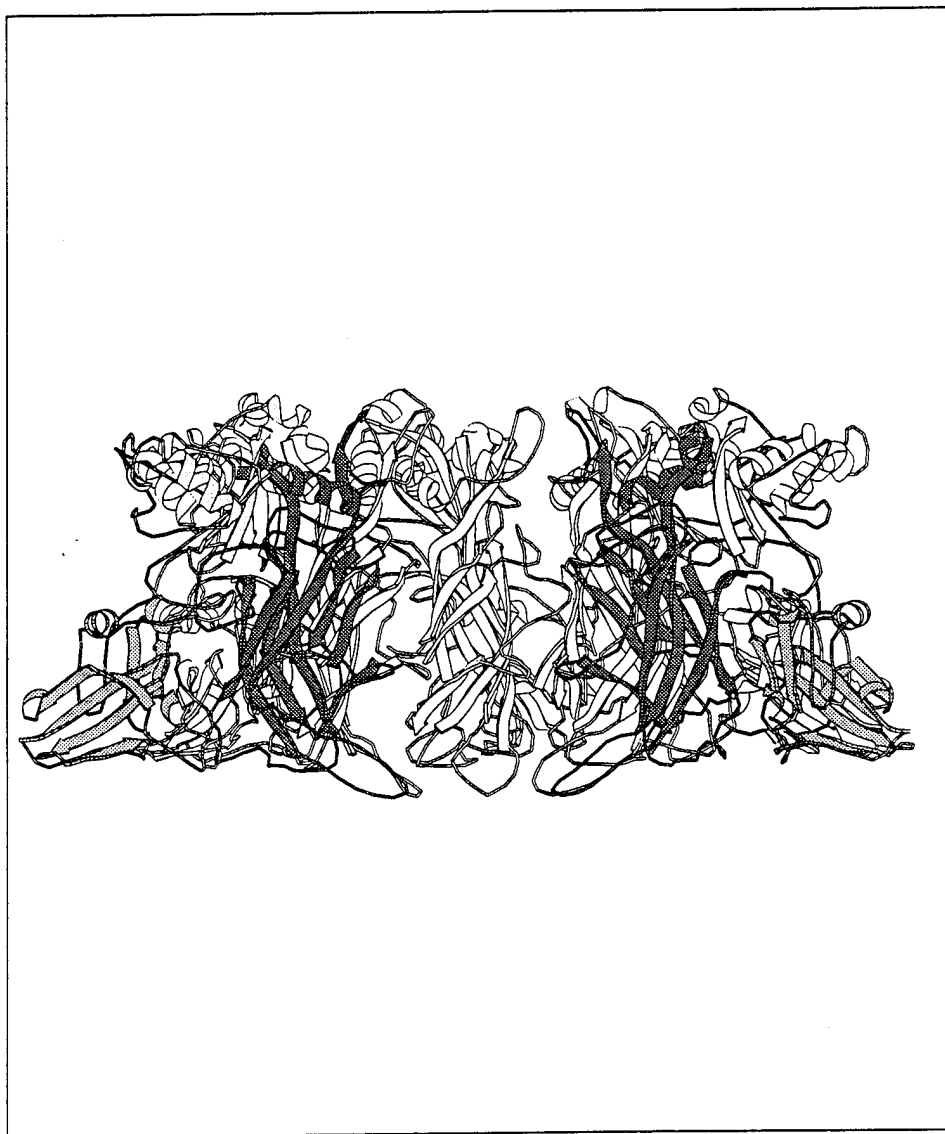


Figure 4b: Hypothetical model of PA63: side view (see text)

phobic residues, a Trp, a Leu and a Met, in the sequence $x_4WxxxMxLx_3$, where x represents a hydrophilic residue. At pH 7.5 these three residues are buried within the core of the β -barrel but become exposed at pH 6 in a disordered loop. We have not yet established that this change is pH-induced rather than a consequence of the crystal lattice, but it is tempting to hypothesize that the exposure of hydrophobic residues represents a step in pH-induced membrane insertion. Interestingly, the corresponding sequence in iota-Ib ($x_4WxxxLxIx_3$) displays a similar pattern of amphipathicity.

axis of 7-fold rotational symmetry, with domain 2 likely facing the channel interior and domains 3 and 4 facing outward. A hypothetical model of the heptamer is shown in figure 4. The loops of domain 2 implicated in oligomerization face the exterior, such that an interaction with the hydrophobic patch of domain 3 from a neighbouring molecule is feasible. The WxxxMxL stretch possibly involved in membrane insertion and the receptor-binding domain are located at the bottom of the heptamer in figure 4b, and the residues suspected of binding EF and LF are at the top. We therefore imagine the membrane to be oriented horizontally at the bottom of figure 4b, such that membrane insertion, possibly accompanied by lateral separation of the receptor-binding domain, would leave the putative EF/LF binding site exposed to the extracellular environment, consistent with the ability of EF/LF to block the conductance of membrane channels formed by PA₆₃ (41).

We repeat that this is still a hypothetical model, and that confirmation requires a full crystallographic analysis of the heptamer. We have obtained crystals that diffract to 4.5Å resolution, so that, together with the high resolution structure of the monomeric PA, we should be able to build an accurate model of the heptamer in the near future.

CONCLUSIONS

The work described in this report defines for the first time the atomic resolution structure of the major antigenic component of the anthrax toxin, the 'protective antigen', revealing that the molecule comprises four distinct domains. Together with existing biochemical and genetic data, we can now begin to assign functions to each domain, although some of these assignments must remain speculative until the crystal structure of the oligomeric PA63 has been determined.

A number of suggestions for directions to an improved vaccine immediately suggest themselves. For example, our crystallographic results and the biochemical data from other groups lead to the assignment of Domain 4 as the 'receptor-binding' domain; our precise definition of the residues comprising this domain will allow it to be expressed as a recombinant protein and tested for its immunogenic and protective properties. The sequence between residues 310-324 forms a large disordered loop that may be required for oligomerization to form PA63. Mutations in this loop that prevent oligomerization could produce a defective PA molecule that was otherwise normally immunogenic (53). Our data also suggest a range of mutations that can be used to test the functional role of other residues on the protein surface.

The work on the full-length protective antigen molecule is now nearly complete, ahead of schedule from our original estimate. We will now focus on the structure of the oligomeric PA63 molecule, which is progressing on schedule. We will also take this opportunity to extend the work to the Lethal Factor (LF) protein. We have crystals of the full length LF that diffract to better than 3Å; also the N-terminal domain of LF (LF_N) is available as a recombinant fragment, and we will attempt crystallization of this fragment, both by itself and in complex with PA63, allowing us to define the molecular interface between PA63 and LF. The success of chimeric LF molecules in translocating foreign molecules into the cytoplasm suggests that this information will be also of use in the generation of targeted toxins (62).

REFERENCES

1. Hambleton P, Turnbull PCB. Anthrax vaccine development: a continuing story. In: Mizrahi A. Bacterial vaccines. Advances in Biotechnological Processes, Vol 13. New York:Alan R.Liss, 1990:105-22.
2. Christie AB. Infectious diseases: epidemiology and clinical practice. IVth edition. Edinburgh: Churchill Livingstone, 1987:983.
3. Bell JH. on anthrax and anthracaemia in woolsorters, heifers and sheep. Br Med J 1880;2:656.
4. La Force FM. Woolsorters' disease in England. NY Acad Med 1978;54:956.
5. Albrink WS, Brooks SM, Biron RE, Kopel M. Human inhalation anthrax: a report on three cases. Am J Pathol 1960;36:457.
6. Koch R. The aetiology of anthrax based on the ontogeny of the anthrax bacillus. Beitr Biol Pflanz 1877;2:277.
7. Leppla, S.H. Anthrax toxins. In: Moss J, Iglewski B, Vaughan M, Tu AT, ed. Bacterial Toxins and Virulence Factors in Disease. New York:Marcel Dekker, 1995: 543-72.
8. Pezard C, Berche P, Mock, M. Contribution of individual toxin components to virulence of *Bacillus anthracis*. Infect Immun 1991; 59:3472-3477.
9. Fish DC, Klein F, Lincoln RE, Walker JS, Dobbs JP. Pathophysiological changes in the rat associated with anthrax toxin.J Infect Dis 1968; 118:114-24.
10. Beall FA, Taylor MJ,Thorne CB. Rapid lethal effect in rats of a third component found upon fractionating the toxin of *Bacillus anthracis*. J Bacteriol 1962;83:1274-80.
11. Smith H, Stoner HB. Anthrax toxic complex. Fed Proc 1967;26:1554-1557.
12. Leppla SH. The anthrax toxin complex. In: Alouf JE, Freer, JH, ed. Sourcebook of Bacterial Protein Toxins. San Diego:Academic Press, 1991:277-302.
13. Friedlander AM. The anthrax toxins. In: Saelinger C, ed.Trafficking of Bacterial Toxins. CRC Press: Boca Raton, 1990:121-28.
14. Stephen J. Anthrax toxin. Pharm Therap 1991;12:501-513.
15. Turnbull PC. Anthrax vaccines: past, present, and future. Vaccine 1991;9:533-39.
16. Abramova FA, Grinberg LM, Yamporskaya OV, Walker DH. Pathology of inhalational anthrax in 42 cases from the Sverdlovsk outbreak of 1979. Proc Natl Acad Sci USA 1993; 90:2291-94.
17. Meselson M, Guillemin J, Hugh-Jones M, Langmuir A, Popova I, Shelokov A, Yampolskaya O. The Sverdlovsk anthrax outbreak of 1979. Science 1994;266:1202-8.

18. Friedlander AM. Macrophages are sensitive to anthrax lethal toxin through an acid-dependent process. *J Biol Chem.*1986;261:7123-26.
19. Considine R, Simpson L. Cellular and molecular action of binary toxins possessing ADP-ribosyltransferase activity. *Toxicon* 1991;29:913-36.
20. Welkos SL, Lowe JR, Eden-McCutchan F, Vodkin M, Leppla SH, Schmidt JJ. Sequence and analysis of the DNA encoding protective antigen of *Bacillus anthracis*. *Gene* 1988;69:287-300.
21. Escuyer V, Duflot E, Sezer O, Danchin A, Mock M. (1988). Structural homology between virulence-associated bacterial adenylate cyclases. *Gene* 1988;71:293-98.
22. Robertson DL, Tippetts MT, Leppla SH. Nucleotide sequence of the *Bacillus anthracis* edema factor gene (*cya*): a calmodulin-dependent adenylate cyclase. *Gene* 1988;73:363-71.
23. Bragg TS, Robertson DL. Nucleotide sequence and analysis of the lethal factor gene (*lef*) from *Bacillus anthracis*. *Gene* 1989; 81:45-54.
24. Hanna PC, Acosta D, Collier RJ. On the role of macrophages in anthrax. *Proc Natl Acad Sci USA* 1993;90:10198-201.
25. Hanna PC, Kochi, S, Collier RJ. Biochemical and physiological changes induced by anthrax lethal toxin in J774 macrophage-like cells. *Mol Biol Cell.*1992;3:1269-77.
26. Hanna PC, Kruskal BA, Ezekowitz RAB, Bloom BR, Collier RJ. Role of macrophage oxidative burst in the action of anthrax lethal toxin. *Molecular Medicine* 1994;1:7-18.
27. Escuyer V, Collier RJ. Anthrax protective antigen interacts with a specific receptor on the surface of CHO-K1 cells. *Infect Immun* 1991; 59:3381-86.
28. Klimpel KR, Molloy SS, Thomas G, Leppla SH. Anthrax toxin protective antigen is activated by a cell surface protease with the sequence specificity and catalytic properties of furin. *Proc Natl Acad Sci USA* 1992;89:10277-81.
29. Molloy SS, Bresnahan PA, Leppla SH, Klimpel KR, Thomas G. Human furin is a calcium-dependent serine endoprotease that recognizes the sequence Arg-X-X-Arg and efficiently cleaves anthrax toxin protective antigen. *J Biol Chem* 1992;267:16396-16402.
30. Gordon VM, Klimpel KR, Arora N, Henderson MA, Leppla SH. (1995). Proteolytic activation of bacterial toxins by eukaryotic cells is performed by furin and by additional cellular proteases. *Infect Immun* 1995;63:82-87.
31. Leppla SH, Friedlander AM, Cora EM. Proteolytic activation of anthrax toxin bound to cellular receptors. In: Fehrenbach FJ, Alouf JE, Falmagne P, Goebel W,

- Jeljaszewicz J, Jurgen D, Rappuoli, R, ed. Bacterial Protein Toxins. New York: Gustav Fischer, 1988:111-2.
32. Gordon VM, Leppla SH, Hewlett EL. Inhibitors of receptor-mediated endocytosis block the entry of *Bacillus anthracis* adenylate cyclase toxin but not that of *Bordetella pertussis* adenylate cyclase toxin. Infect Immun 1988;56:1066-69.
 33. Leppla SH. Anthrax toxin edema factor: a bacterial adenylate cyclase that increases cyclic AMP concentrations in eukaryotic cells. Proc Natl Acad Sci USA 1982; 79:3162-66.
 34. Klimpel KR, Arora N, Leppla SH. Anthrax toxin lethal factor contains a zinc metalloprotease consensus sequence which is required for lethal toxin activity. Mol Microbiol 1994;13:1093-1100.
 35. Milne JC, Furlong D, Hanna PC, Wall JS, Collier RJ. (1994). Anthrax protective antigen forms oligomers during intoxication of mammalian cells. J Biol Chem 1994;269:20607-12.
 36. Blaustein RO, Koehler TM, Collier RJ, Finkelstein A. Anthrax toxin: channel-forming activity of protective antigen in planar phospholipid bilayers. Proc Natl Acad Sci USA 1989; 86: 2209-13.
 37. Finkelstein A. The channel formed in planar lipid bilayers by the protective antigen component of anthrax toxin. Toxicology 1994;87:29-41.
 38. Koehler TM, Collier RJ. (1991). Anthrax toxin protective antigen: low pH-induced hydrophobicity and channel formation in liposomes. Mol Microbiol 1991; 5:1501-1506.
 39. Milne, J.C. and Collier, R.J. pH-dependent permeabilization of the plasma membrane of mammalian cells by anthrax protective antigen. Mol Microbiology 1993;10:647-653.
 40. Finkelstein A. Channels formed in phospholipid bilayer membranes by diphtheria, tetanus, botulinum, and anthrax toxin. J Physiol (Paris) 1990; 84:188-90.
 41. Zhao J, Milne JC, Collier RJ. Effect of anthrax toxin's LF component on ion channels formed by the PA component. J Biol Chem 1995; in press.
 42. Blaustein RO, Finkelstein A. (1990a). Diffusion limitation in the block by symmetric tetraalkylammonium ions of anthrax toxin channels in planar phospholipid bilayer membranes. J Gen Physiol 1990;96:943-57.
 43. Blaustein RO, Finkelstein A. Voltage-dependent block of anthrax toxin channels in planar phospholipid bilayer membranes by symmetric tetraalkylammonium ions. J Gen Physiol 1990; 96:905-19.

44. Blaustein RO, Finkelstein A. Voltage-dependent block of anthrax toxin channels in planar phospholipid bilayer membranes by symmetric tetraalkylammonium ions. Effects on macroscopic conductance. *J Gen Physiol* 1990; 96:921-42.
45. Terwilliger, T. and Eisenberg, D. (1983). Unbiased three-dimensional refinement of Heavy atom parameters by correlation of origin-removed Patterson coefficients. *Acta Cryst.* A39 , 813-817.
46. Otwinowski, Z. (1991) Maximum likelihood refinement of heavy atom parameters. *In* Proceedings of the CCP4 Study Weekend: Isomorphous Replacement and Anomalous Scattering, Daresbury Laboratory, 80-85.
47. Jones, T.A. (1978) A graphics model building and refinement system for macromolecules. *J.Apply. Cryst.* 11, 268-272.
48. Bruenger, A.T. (1992) *X-PLOR Manual version 3.1*. Yale University, New Haven, CT.
- 49 .Read, R.J. (1986) Improved Fourier coefficients for maps using phases from partial structures with errors. *Acta Cryst. A* 42, 140-149.
50. Zhang,K.Y.J. (1993) SQUASH - combining constraints for macromolecular phase refinement and extension. *Acta Cryst. D* 49, 213-222.
51. Novak JM, Stein M-P, Little SF, Leppla SH, Friedlander AM. Functional characterization of protease-treated *Bacillus anthracis* protective antigen. *J Biol Chem* 1992;267:17186-93.
52. Singh Y, Chaudhary VK, Leppla SH. A deleted variant of *Bacillus anthracis* protective antigen is non-toxic and blocks anthrax toxin *in vivo*. *J Biol Chem* 1989;264:19103-7.
53. Singh Y, Klimpel KR, Arora N, Sharma M, Leppla SH. The chymotrypsin-sensitive site, FFD³¹⁵, in anthrax toxin protective antigen is required for translocation of lethal factor. *J Biol Chem* 1994;269:29039-46.
54. Singh Y, Klimpel KR, Quinn CP, Chaudhary VK, Leppla SH. The carboxyl-terminal end of protective antigen is required for receptor binding and anthrax toxin activity. *J Biol Chem* 1991; *Journal of Biological Chemistry* 266:15493-15497.
55. Little SF, Lowe JR. Location of receptor-binding region of protective antigen from *Bacillus anthracis*. *Biochem Biophys Res Commun* 1991;180:531-537.
56. Perelle, S, Gibert M, Boquet P, Popoff MR. Characterization of *Clostridium perfringens* iota-toxin genes and expression in *Escherichia coli*. *Infect Immun* 1993;61:5147-5156.
57. Stiles, BG, Wilkins TD. *Clostridium perfringens* iota toxin: synergism between two proteins. *Toxicon* 1986;24:767-773.

58. Stiles BG, Wilkins TD. Purification and characterization of *Clostridium perfringens* iota toxin: dependence on two non-linked proteins for biological activity. Infect Immun 1986;54:683-88.
59. Simpson, L.L., Stiles, B.G., Zepeda, H.H. and Wilkins, T.D. (1987). Molecular basis for the pathological actions of *Clostridium perfringens* iota toxin. Infect Immun.1987; 55:118-22.
60. Vandekerckhove J, Schering B, Barmann M, Aktories K. *Clostridium perfringens* iota toxin ADP-ribosylates skeletal muscle actin in Arg-177. FEBS Lett 1987;225:48-52.
61. Popoff MR, Milward FW, Bancillon B, Boquet P. Purification of the *Clostridium spiroforme* binary toxin and activity on HEp-2 cells. Infect Immun 1989;57:2462-69.
62. Pastan I, Chaudhary V, Fitzgerald DJ. Recombinant toxins as novel therapeutic agents. Ann Rev Biochem 1992;61:331-54.

BIBLIOGRAPHY

Personnel receiving pay: Robert Liddington, Ph.D., Jadwiga Bienkowska, Ph.D,
João Cabral, Ph.D.

Publications and Meeting Abstracts: None